S1 Analysis using wavelets: time-frequency

Analysis using wavelets overcomes limitations of the classical Fourier analysis and is well suited for non-stationary signals such as hydrologic signals (Labat, 2005). Wavelet transform utilizes basic functions called wavelets to transform a signal into its constituent frequencies while providing time localization. Signal decomposition is accomplished through wavelets, which are applied as a bandpass filter (Grinsted et al., 2004). The complex non-orthogonal Morlet wavelet is a complex exponential (sinusoidal function) modulated by a Gaussian envelope which ensures time localization and is described as shown in Eq. S1 (Anctil et al., 2008;Addison, 2005).

$$\psi_0(\eta) = \pi^{\frac{-1}{4}}\left(e^{i\omega_0\eta} - e^{\frac{\omega_0^2}{2}}\right)e^{\frac{-\eta^2}{2\sigma^2}}, \quad \text{(S1)}$$

where, $\psi_0(\eta)$ is the wavelet function, also called the mother wavelet. Similar to the classical version of the Heisenberg's uncertainty principle, if we want a precise characterization of frequency, we cannot precisely locate the frequency in time and vice versa (Farge et al., 1990;Labat, 2005). The ω_0 set at 6, provides a good balance between time and frequency localization (Grinsted et al., 2004). The second term in Eq. (1) is a correction factor to satisfy the admissibility criteria of zero mean or no non-zero frequency and for $\omega_0 = 6$, $e^{\frac{\omega_0^2}{2}}$ becomes so small that it can be neglected (Addison, 2005). It also refers to the number of cycles in the wavelet. η is non-dimensional time parameter which is defined as $(n' - n)\delta t$, σ^2 is the measure of support and is set as 1. Complex Morlet is also ideal for feature extraction (Anctil et al., 2008).

The continuous wavelet transform (CWT), $W_n^x(s)$, is defined as the convolution of a discrete sequence (real signal) x_n, $n = 1, 2, 3 \ldots N$, where N is the length of the time series, with the scaled and translated version of the mother wavelet function, $\psi_0(\eta)$ (see Eq. S2) (Anctil et al., 2008).

$$W_n^x(s) = \sqrt[2]{\frac{\delta t}{s}}\sum_{n'=0}^{N-1} x_{n'}\psi_0\left[\frac{(n'-n)\delta t}{s}\right] \quad \text{(S2)}$$

where, $W_n^x(s)$ is the complex wavelet transform, s is a dimensionless variable called the scale dilation parameter and corresponds to the width of the wavelet with $s \in \mathbb{R}^+$, n is also a dimensionless variable called the translational parameter and corresponds to the actual position of the wavelet in the physical space with $s \in \mathbb{R}^n$, δt is the sampling time step, $\sqrt[2]{\frac{\delta t}{s}}$ is the normalization factor which causes all wavelets (corresponding to each scale) to have the same L^2 norm resulting in same energy. The CWT matrix contains an estimate of the instantaneous hydrologic response that is influenced by neighboring activity. $|W_n^x(s)|$ is the modulus of the CWT also called the amplitude (Liu, 1994). The univariate CWT can be extended to compare two signals x_n and y_n in the context of wavelet analysis to obtain regions of high common power and can be estimated with the cross wavelet transform, $W_n^{xy}(s)$, as defined in Eq. S3 (Liu et al., 2011).

$$W_n^{xy}(s) = W_n^x(s)W_n^{y*}(s) \quad \text{(S3)}$$

where, * denotes the complex conjugate.

Wavelet coherence, $R_n^2(s)$, can be used to identify the scales and time periods where the two signals are similar. The squared modulus of the cross wavelet transform normalized by the product of the wavelet transforms of the individual signals results in the wavelet coherence (Schaefli et al., 2007). It is a measure analogous to the coefficient of determination in statistics and can be used to compare any two signals and is defined as shown in Eq. S4 (Liu et al., 2011).

$$R_n^2(s) = \frac{\left|\langle s^{-1} W_n^{xy}(s)\rangle\right|^2}{\langle s^{-1}|W_n^x(s)|^2\rangle \cdot \langle s^{-1}|W_n^y(s)|^2\rangle} \quad \text{(S4)}$$

S2 Model performance using R^2 and PBIAS

In Fig. S3 (a), (b) and (c), we see that R^2 captures regions similar to NSE as desired solutions. In Figure 4 (a) and (b), we see that PBIAS also captures regions similar to R^2 as desired solutions. Percent Bias (PBIAS) is the error in the model prediction normalized by the measured stream flow. The ideal value for PBIAS is zero, with positive values indicating over prediction and negative values indicating under prediction. For easier comparison, Figure 4 (a-c) PBIAS values are shown as absolute values to stay consistent with cooler colors as desired solutions. Here closer to zero values are ideal solutions. Similar to NSE and R^2, PBIAS fails to narrow the parameter space. A multi-objective criterion may not fully resolve the challenges with equifinality.

References

Addison, P. S.: Wavelet transforms and the ECG: a review, Physiological Measurement, 26, R155, 2005.

Anctil, F., Pratte, A., Parent, L., and Bolinder, M.: Non-stationary temporal characterization of the temperature profile of a soil exposed to frost in south-eastern Canada, Nonlinear Processes in Geophysics, 15, 409, 2008.

Farge, M., Guezennec, Y., Ho, C., and Meneveau, C.: Continuous wavelet analysis of coherent structures, Proceedings of the 1990 Summer Program, 1990, 331-348,

Grinsted, A., Moore, J. C., and Jevrejeva, S.: Application of the cross wavelet transform and wavelet coherence to geophysical time series, Nonlinear Processes in Geophysics, 11, 561-566, 2004.

Labat, D.: Recent advances in wavelet analyses: Part 1. A review of concepts, Journal of Hydrology, 314, 275-288, http://dx.doi.org/10.1016/j.jhydrol.2005.04.003, 2005.

Liu, P. C.: Wavelet spectrum analysis and ocean wind waves, Wavelets in geophysics, 4, 151-166, 1994.

Liu, Y., Brown, J., Demargne, J., and Seo, D.-J.: A wavelet-based approach to assessing timing errors in hydrologic predictions, Journal of Hydrology, 397, 210-224, http://dx.doi.org/10.1016/j.jhydrol.2010.11.040, 2011.

Schaefli, B., Maraun, D., and Holschneider, M.: What drives high flow events in the Swiss Alps? Recent developments in wavelet spectral analysis and their application to hydrology, Advances in Water Resources, 30, 2511-2525, http://dx.doi.org/10.1016/j.advwatres.2007.06.004, 2007.

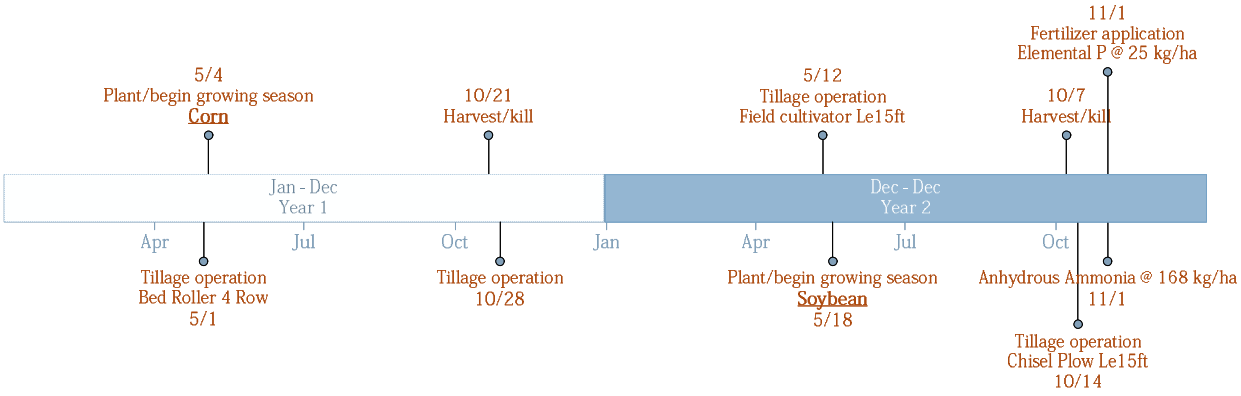

Fig. S1. Scheduling of management operations under corn-soybean rotation in Le Sueur River Basin (LSRB) and are typical management practices that occur within the LSRB. The schedule shown is for HRUs that are initialized with corn as land use. HRUs with soybean as the land use for the 1st year will have the management operations from year 2 as year 1 operation and year 1 as year 2.

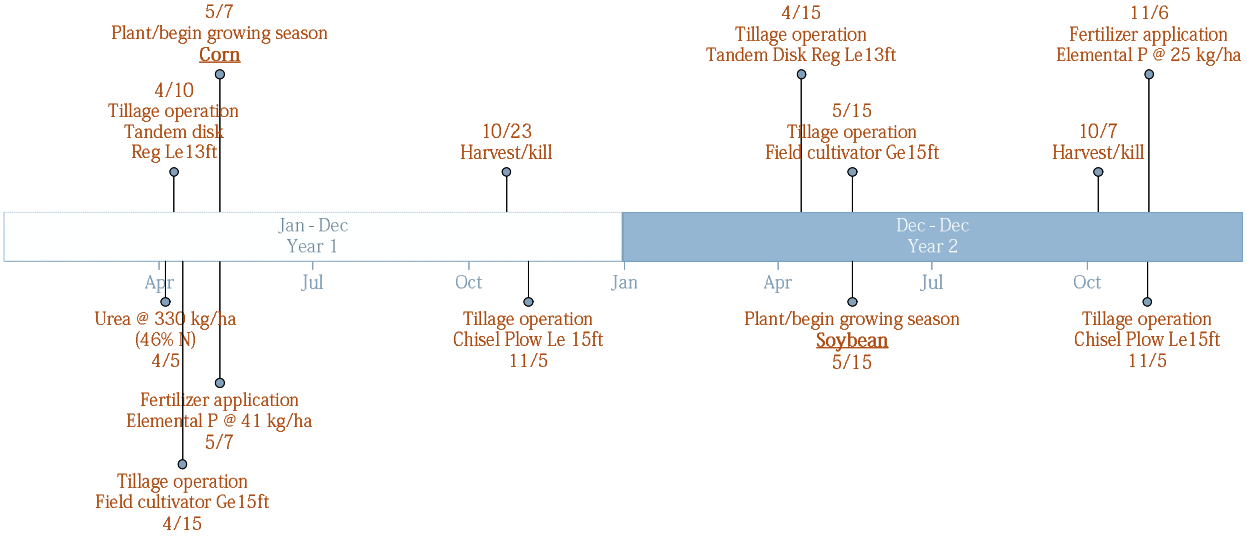

Fig. S2. Scheduling of management operations under corn-soybean rotation in the Root River Basin (RRB) and are typical management practices that occur within the RRB. The schedule shown is for HRUs that are initialized with corn as land use. HRUs with soybean as the land use for the 1st year will have the management operations from year 2 as year 1 operation and year 1 as year 2.

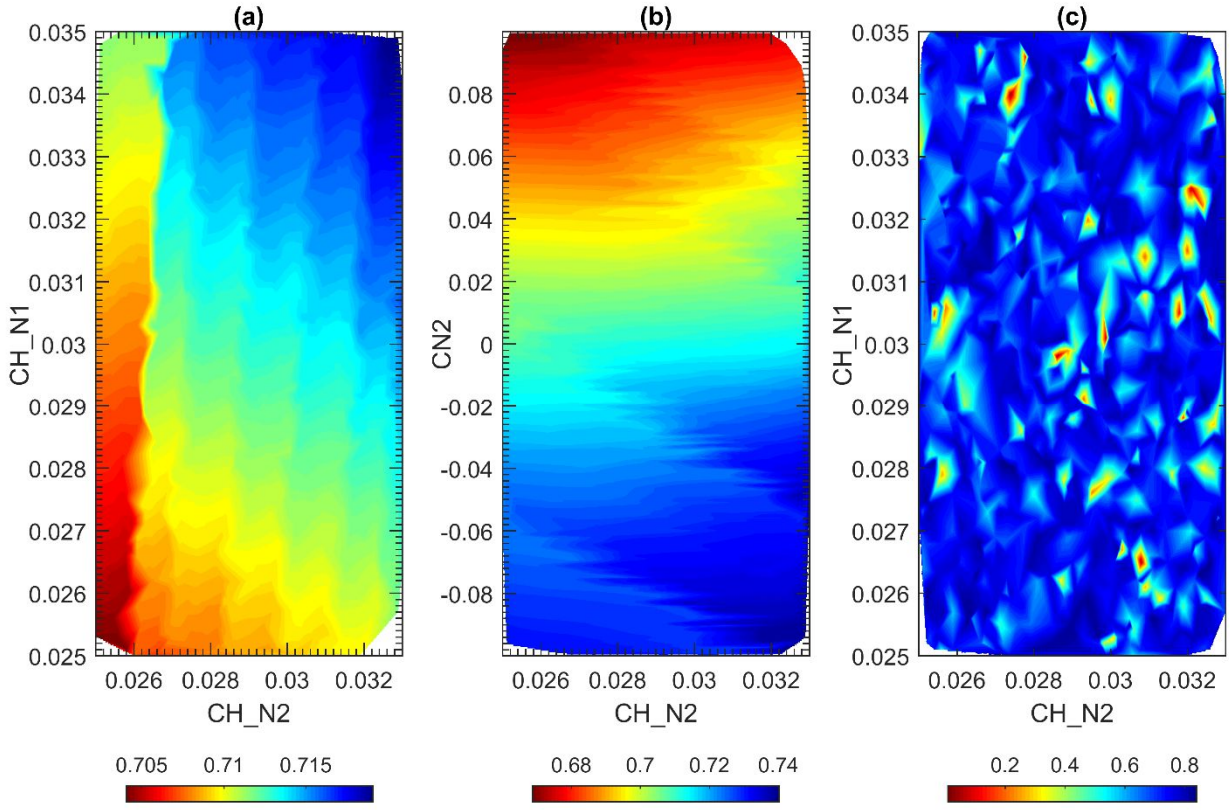

Fig. S3. (a), (b) and (c) were generated from 1000 runs each using the SWAT model for the South Branch of the Root River (sub-model of the Root River SWAT model with same parametrization as the larger RRW model. (a) Contour plot of R^2 (coded as color) value for Manning's "n" value for the tributary channels (CH_N1) and Manning's "n" value for the main channel (CH_N2). (b) Contour plot of NSE value for Curve Number (CN2) and Manning's "n" value for the main channel (CH_N2). (a) Contour plot of NSE value for Manning's "n" value for the tributary channels (CH_N1) and Manning's "n" value for the main channel (CH_N2) when 18 parameters were varied.

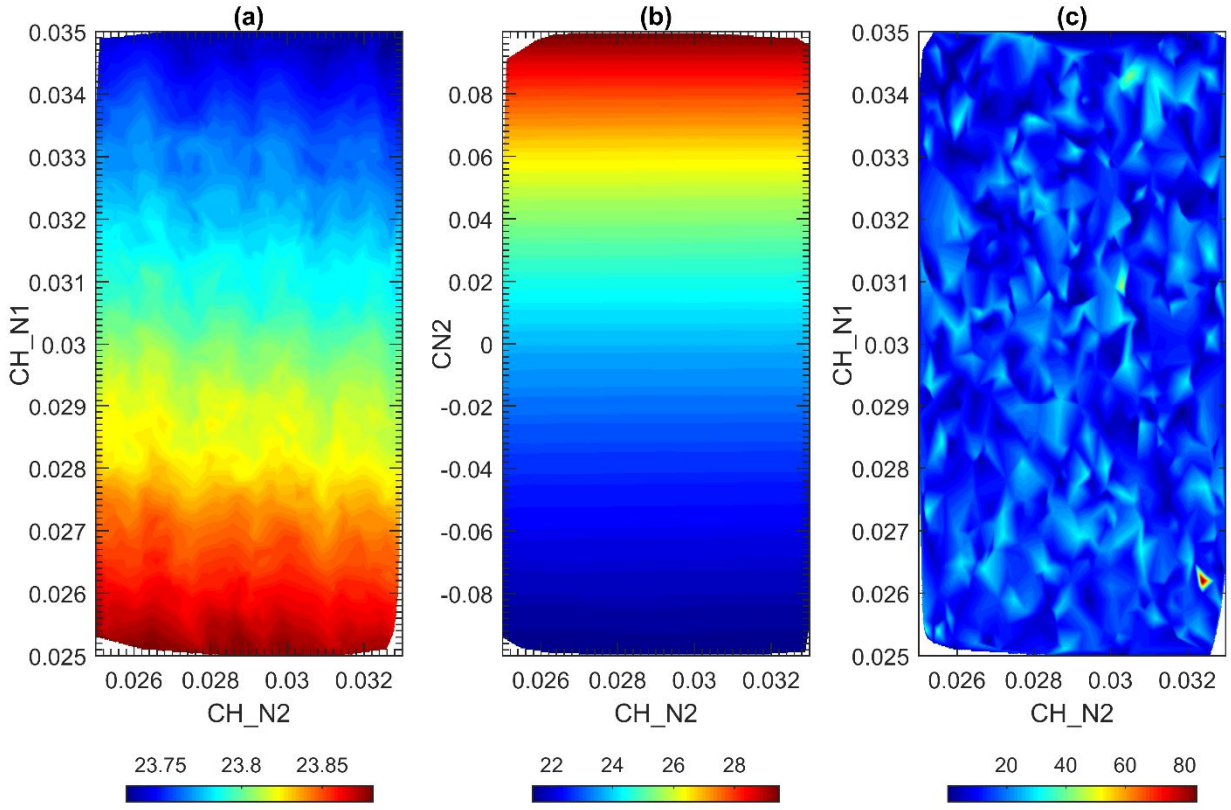

Fig. S4. (a), (b) and (c) were generated from 1000 runs each using the SWAT model for the South Branch of the Root River (sub-model of the Root River SWAT model with same parametrization as the larger RRW model. (a) Contour plot of PBIAS (coded as color) value for Manning's "n" value for the tributary channels (CH_N1) and Manning's "n" value for the main channel (CH_N2). (b) Contour plot of NSE value for Curve Number (CN2) and Manning's "n" value for the main channel (CH_N2). (a) Contour plot of NSE value for Manning's "n" value for the tributary channels (CH_N1) and Manning's "n" value for the main channel (CH_N2) when 18 parameters were varied.

Table S1. List of 18 SWAT model parameters that were adjusted to illustrate numerous local maxima.

Parameter	Range (min.)	Range (max.)
ALPHA_BF.gw	0	1
GW_DELAY.gw	1	450
GWQMN.gw	1	1000
CH_N2.rte	0.025	0.033
CH_K2.rte	0	100
CH_N1.sub	0.025	0.035
CH_K1.sub	0	100
SFTMP.bsn	2.3	2.4
SMTMP.bsn	-1	1
SMFMX.bsn	3	4
SMFMN.bsn	2	3
TIMP.bsn	0.4	0.6
SNOCOVMX.bsn	0	10
SNO50COV.bsn	0	0.5
ESCO.bsn	0.5	1
EPCO.bsn	0	0.3
CNCOEF.bsn	0.5	0.8
CN_FROZ.bsn	0.001	0.003

Table S2. List of SWAT model parameters that were calibrated for the Le Sueur River Basin (LSRB) along with their classification into the three sets. Only pure and derived calibration parameters were adjusted.

Parameter	Adjustment status	Description	SWAT Default value	Calibrated value	Calibrated Range
.bsn file - General watershed description file					
SFTMP	P	Snowfall temperature (°C)	1	2.2	NA
SMTMP	P	Snow melt base temperature (°C)	0.5	0.5	NA
SMFMX	P	Melt factor for snow on June 21 (mm H_2O/°C-day)	4.5	4	NA
SMFMN	P	Melt factor for snow on December 21 (mm H_2O/°C-day)	4.5	2	NA
TIMP	P	Snow pack temperature lag factor	1	0.815	NA
SNOCOVMX	P	Minimum snow water content that corresponds to 100% snow over (mm H_2O)	1	10	NA
SNO50COV	P	Fraction of snow volume represented by SNOCOVMC that corresponds to 50% snow cover	0.5	0.5	NA
IPET	P*	Potential evapotranspiration (PET) method	Penman/Monteith	Hargreaves	NA
ESCO	P	Soil evaporation compensation factor	0.95	0.98	NA
EPCO	P	Plant uptake compensation factor	1	0.005	NA
ICN	P*	Daily curve number calculation method	Soil Moisture Method	Plant ET Method	NA
CNCOEF	P	Plant ET curve number coefficient	1	0.7	NA
CN_FROZ	P	Frozen soil infiltration factor	0 .000862, "inactive"	0.002, "active"	NA
ITDRN		Tile drain equation flag	0	1	NA
IWTDN		Water table algorithm flag	0	1	NA
.gw file - Groundwater input file					
GW_DELAY	P	Groundwater delay time (days)	31	42.63	NA
ALPHA_BF	P	Baseflow alpha factor (1/days)	0.048	0.83	NA
GWQMN	P	Threshold depth of water in the shallow aquifer required for return flow to occur (mm H_20)	1000	1359.61	NA
GW_REVAP	P	Groundwater revap coefficient	0.02	0.047	NA
.sub file - Subbasin general input file					
CH_N1	D	Mannings "n" value for tributary channel	0.014	0.04	NA
CH_K1	D	Effective hydraulic conductivity in tributary channel alluvium (mm/hr)	0	30.9	NA
.rte file – Main channel input file					
CH_N2	P	Mannings "n" value for main channel	0.014	0.037	NA
CH_K2	P	Effective hydraulic conductivity in main channel alluvium (mm/hr)	0	171.3	NA
.hru file – HRU general input file					

DEP_IMP	P	Depth to impervious layer in soil profile (mm)	NA	2237.17	NA
RE	D	Effective radius of drains (mm)	50	25	NA
SDRAIN	P	Distance between two drains or tile tubes (mm)	NA	NA	15000 - 18200
OV_N	D	Manning's "n" value for overland flow	-999	0.03	NA

- NA – Not Applicable
- P – Pure calibration parameter
- P* – Model structure. Considered as pure calibration parameter.
- D – Derived calibration parameter
- Scheduling: In theory it is knowable or measurable information, but in reality it is hard to obtain on the scale of a large watershed (> 2000 km^2). It is specified as a measured parameter in this paper.

Table S3. List of SWAT model parameters that were calibrated for the Root River Basin (RRB). along with their classification into the three sets. Only pure and derived calibration parameters were adjusted.

Parameter	Adjustment status	Description	SWAT Default value	Calibrated value	Calibrated Range
.bsn file - General watershed description file					
SFTMP	P	Snowfall temperature (°C)	1	2.35	NA
SMTMP	P	Snow melt base temperature (°C)	0.5	0.14	NA
SMFMX	P	Melt factor for snow on June 21 (mm H_2O/°C-day)	4.5	3.41	NA
SMFMN	P	Melt factor for snow on December 21 (mm H_2O/°C-day)	4.5	2.54	NA
TIMP	P	Snow pack temperature lag factor	1	0.53	NA
SNOCOVMX	P	Minimum snow water content that corresponds to 100% snow over (mm H_2O)	1	4.35	NA
SNO50COV	P	Fraction of snow volume represented by SNOCOVMC that corresponds to 50% snow cover	0.5	0.27	NA
IPET	P*	Potential evapotranspiration (PET) method	Penman/Monteith	Hargreaves	NA
ESCO	P	Soil evaporation compensation factor	0.95	0.81	
EPCO	P	Plant uptake compensation factor	1	0.19	
ICN	P*	Daily curve number calculation method	Soil Moisture Method	Plant ET Method	NA
CNCOEF	P	Plant ET curve number coefficient	1	0.61	NA
CN_FROZ	P	Frozen soil infiltration factor	0 .000862, "inactive"	0.00167, "active"	NA
.gw file - Groundwater input file					
GW_DELAY	P	Groundwater delay time (days)	31	NA	1.2 - 456.7
ALPHA_BF	P	Baseflow alpha factor (1/days)	0.048	NA	0.58 - 1.0
GWQMN	P	Threshold depth of water in the shallow aquifer required for return flow to occur (mm H_20)	1000	NA	1.6 - 1214.6
.sub file - Subbasin general input file					
CH_N1	P	Mannings "n" value for tributary channel	0.014	NA	0.03 – 0.09
CH_K1	P	Effective hydraulic conductivity in tributary channel alluvium (mm/hr)	0	NA	7.8 – 143.8
.rte file – Main channel input file					
CH_N2	P	Mannings "n" value for main channel	0.014	NA	0.034 – 0.047
CH_K2	P	Effective hydraulic conductivity in main channel alluvium (mm/hr)	0	NA	0.86 – 93.02

- NA – Not Applicable
- P – Pure calibration parameter
- P*– Model structure. Considered as pure calibration parameter.
- D – Derived calibration parameter

- Scheduling: In theory it is knowable or measurable information, but in reality it is hard to obtain on the scale of a large watershed (> 2000 km^2). It is specified as a measured parameter in this paper.